

Non-axisymmetric, scale-free, razor-thin discs

D. Syer^{1,2} and S. Tremaine¹

¹ *Canadian Institute for Theoretical Astrophysics, McLennan Labs, 60 St. George Street, Toronto M5S 3H8, Ontario, Canada.*

² *Max-Planck-Institut für Astrophysik, Karl-Schwarzschild-Straße 1, 85748 Garching-bei-München, Germany.*

ABSTRACT

We develop equations to describe the equilibrium state of razor-thin scale-free barotropic fluid discs, with rotation curve $v \propto R^{-\beta}$, $\beta \in (-\frac{1}{4}, \frac{1}{2})$. The discs may be embedded in a scale-free axisymmetric background potential. Nearly axisymmetric discs are constructed analytically and discs with azimuthal density variations as large as 10:1 are constructed numerically. For small departures from axisymmetry, we find that: (i) Stationary self-consistent cold or cool discs with $m \geq 2$ do not exist; (ii) on a plane whose axes are the Mach number and the strength of the background potential, there are generally two one-parameter sequences of non-axisymmetric discs (one with aligned isodensity contours and one with spiral contours); the spiral sequence exists only for $m = 1$; (iii) isolated discs with a flat rotation curve ($\beta = 0$) support non-axisymmetric equilibrium states at all Mach numbers, and discs with $\beta = \frac{1}{4}$ support a two-parameter family of self-similar spiral patterns.

Key words: hydrodynamics – galaxies: kinematics and dynamics

1 INTRODUCTION

Disc galaxies exhibit a variety of non-axisymmetric structure (bars, spiral structure, lopsided structure, etc.). See Baldwin, Lynden-Bell & Sancisi (1980) and Richter & Sancisi (1994) for an HI survey of asymmetries in the discs of galaxies, and Rix & Zaritsky (1995) for a study of the phenomenon in stellar light. These asymmetries suggest the following general problem: what are the possible stationary configurations of a two-dimensional self-gravitating fluid other than an axisymmetric razor-thin disc? One example is the family of Riemann discs (Weinberg & Tremaine 1983, Weinberg 1983) but these are uniformly rotating and hence only relevant to the central parts of disc galaxies.

In this paper we address a modest component of this problem: we seek non-axisymmetric razor-thin discs of two-dimensional barotropic fluid that are stationary in an inertial frame. We distinguish between ‘razor-thin’ and ‘two-dimensional,’ applying the latter term to the equation of state (see Section 2). Furthermore we assume that our systems are scale-free, which reduces the partial differential equations describing the system to ordinary differential equations. We also allow for the presence of an axisymmetric background potential. This simple and highly idealized problem already exhibits a rich variety of solutions.

In Section 2 we derive the equations of motion. In Section 3 we solve these equations analytically for small departures from axisymmetry, and in Section 4 we construct highly non-axisymmetric discs numerically.

2 THE EQUATIONS OF MOTION

We use ‘razor-thin’ to refer to a disc that has a density

$$\rho(\mathbf{r}) = \Sigma(R, \theta)\delta(z) \quad (1)$$

where (R, θ, z) are cylindrical polar co-ordinates, and $\delta(z)$ is the Dirac δ -function.

We use ‘two-dimensional’ to refer to a fluid in which the pressure Π acts only in a plane. We use a barotropic equation of state of the form

$$\Pi = k\Sigma^\Gamma, \quad (2)$$

where $k \geq 0$, $\Gamma > 0$.

The gravitational potential in the plane of the disc is given by the Poisson integral

$$\Phi(R, \theta) = -G \int \frac{\Sigma(r, \phi) r dr d\phi}{[r^2 + R^2 - 2Rr \cos(\theta - \phi)]^{1/2}}. \quad (3)$$

If the disc is stationary, the velocity field $\mathbf{v} \equiv v_R \hat{\mathbf{e}}_R + v_\theta \hat{\mathbf{e}}_\theta$ satisfies the continuity equation

$$\nabla \cdot (\Sigma \mathbf{v}) = 0 \quad (4)$$

and the Euler equation

$$(\mathbf{v} \cdot \nabla) \mathbf{v} = -\nabla(\Phi + \bar{\Phi} + H) \quad (5)$$

where $\bar{\Phi}$ represents an imposed axisymmetric background potential and H is the enthalpy. In a two-dimensional barotropic fluid the enthalpy is a function of the surface density, $H = H(\Sigma)$.

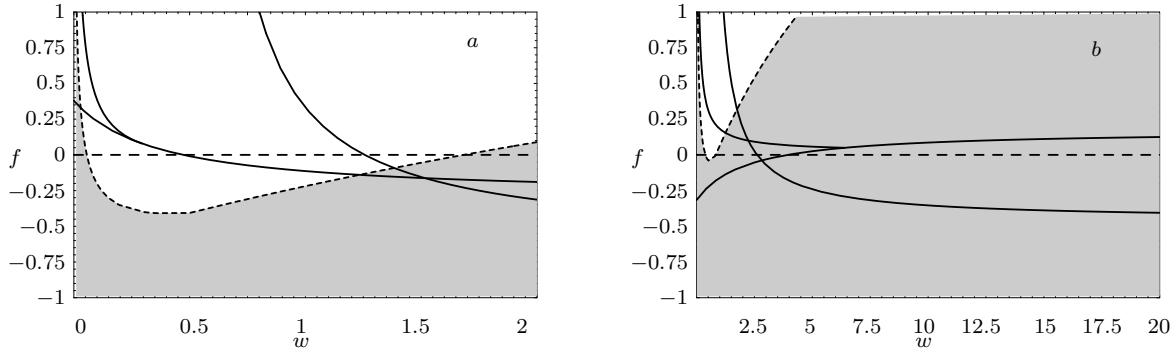


Figure 1. (a) The locus of self-consistent solutions for $\beta = 0.2$, $m = 1$ (two leftmost solid curves) and $m = 2$ (right solid curve); the lower of the two $m = 1$ curves is the family of aligned discs and the upper is the family of spiral discs, which terminates at the bifurcation point $(w, f) = (0.29432, 0.07910)$. The horizontal coordinate w is the inverse square Mach number and the vertical coordinate f is the ratio of the fixed background potential to the unperturbed potential of the disc. For $f < 0$ the background potential is repulsive and hence unphysical; the dashed line $f = 0$ corresponds to an isolated disc with no background potential. In the shaded region, the axisymmetric disc is subject to an $m = 0$ instability. (b) Same as (a), but for $\beta = -0.1$; the bifurcation point at which the $m = 1$ spiral family begins is $(w, f) = (6.38318, 0.04949)$.

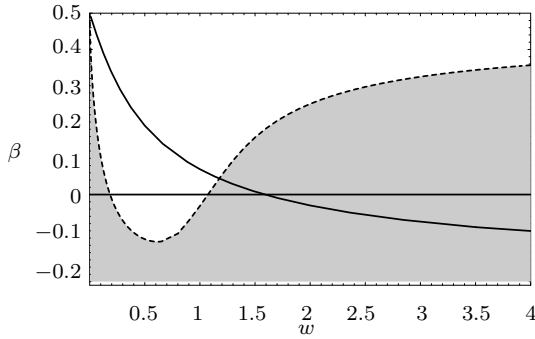


Figure 2. The locus of non-axisymmetric equilibria for isolated discs, $f = 0$ (the solid curve and the solid horizontal line at $\beta = 0$). In the shaded region the axisymmetric disc is subject to an $m = 0$ instability.

We now impose scale-invariance and reduce the two-dimensional partial differential equations to ordinary differential equations. We write

$$\Phi = -R^{-2\beta} P(\varphi), \quad \bar{\Phi} = -R^{-2\beta} \bar{P}, \quad (6)$$

where

$$\varphi(R, \theta) \equiv \theta + \mu \log R, \quad (7)$$

and β and μ are real constants. The disc has a spiral pattern if $\mu \neq 0$; without loss of generality we can assume $\mu \geq 0$.

Equations (3), (4) and (5) can only be satisfied when

$$\Sigma = R^{-2\beta-1} S(\varphi),$$

$$v_R = R^{-\beta} a(\varphi), \quad v_\theta = R^{-\beta} b(\varphi),$$

and

$$H = R^{-2\beta} Q(\varphi).$$

Since we impose scale invariance, all physical quantities are determined by their values on the unit circle $R = 1$. Thus,

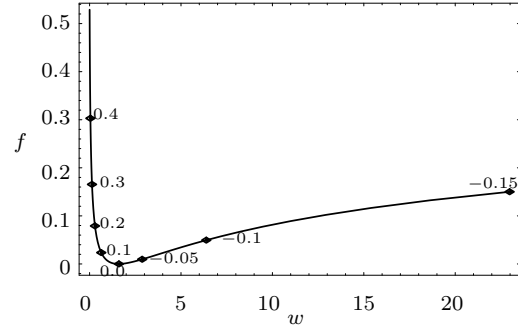


Figure 3. The location of the bifurcation point between the aligned and spiral families of $m = 1$ equilibrium solutions, as a function of β . From left to right, the diamonds mark $\beta = 0.4, 0.3, 0.2, 0.1, 0, -0.05, -0.1, -0.15$. The curve is singular ($w \rightarrow \infty$) at $\beta = -0.2071$, where $f = 0.4381$; in a second branch with $\beta \rightarrow -\frac{1}{2}$ the curve approaches $w \rightarrow 0, f \rightarrow \infty$ but lies beyond the boundary of this figure.

for instance, we shall refer to Σ and S as ‘surface density’ interchangeably.

Mass distributions with $\beta > \frac{1}{2}$ are unphysical because they contain infinite point masses ($\int_r^\infty \Sigma(R, \theta) R dR d\theta \rightarrow \infty$ as $r \rightarrow 0$); we summarise other constraints on β at the end of this section.

The case $\beta = 0$ is special and is most easily handled by taking limits as $\beta \rightarrow 0$, with $P(\varphi) \equiv P_0/(2\beta) + P_1(\varphi)$, $\bar{P} \equiv \bar{P}_0/(2\beta)$, $Q(\varphi) \equiv Q_0/(2\beta) + Q_1(\varphi)$. The result is

$$\begin{aligned} \Phi &= P_0 \log R - P_1(\varphi) + \text{const}, & \bar{\Phi} &= \bar{P}_0 \log R + \text{const}, \\ \Sigma &= \frac{S(\varphi)}{R}, \\ v_R &= a(\varphi), \\ v_\theta &= b(\varphi), \\ H &= -Q_0 \log R + Q_1(\varphi) + \text{const}. \end{aligned} \quad (8)$$

In practice we shall not need these equations, since all the

expressions for physical quantities below are well behaved in the limit $\beta \rightarrow 0$.

The sound speed v_s is given by

$$v_s^2 = \frac{d\Pi}{d\Sigma} = k\Gamma\Sigma^{\Gamma-1}. \quad (9)$$

The enthalpy is given by

$$H = \int \frac{d\Pi}{\Sigma} = k \frac{\Gamma}{\Gamma-1} \Sigma^{\Gamma-1}. \quad (10)$$

To preserve scale-invariance we require that

$$\Gamma = \frac{1+4\beta}{1+2\beta}; \quad (11)$$

the constraint $\Gamma > 0$ implies $\beta > -\frac{1}{4}$. Equation (10) thus implies that

$$Q(\varphi) = \frac{\Gamma}{\Gamma-1} k S(\varphi)^{\Gamma-1} = \frac{1+4\beta}{2\beta} k S(\varphi)^{2\beta/(2\beta+1)}, \quad (12)$$

Equations (3), (4) and (5) can be written

$$P(\varphi) = G \int_0^{2\pi} \frac{S(\chi) y^{-2\beta} dy d\chi}{[1+y^2-2y\cos(\varphi-\chi-\mu\log y)]^{1/2}}, \quad (13)$$

$$3\beta Sa - \mu(Sa)' - (Sb)' = 0, \quad (14)$$

$$2\beta(P + \bar{P} - Q) - \mu(P - Q)' - \beta a^2 - b^2 + \mu a a' + a' b = 0, \quad (15)$$

and

$$(P - Q)' + (\beta - 1)ab - bb' - \mu ab' = 0, \quad (16)$$

where a dash denotes a derivative with respect to φ . Using the equation of state (12) to eliminate Q , these four equations are to be solved for the four functions P , S , a and b .

The allowable range of β is constrained by the convergence of Poisson's equation (3). Let us assume that $S(\varphi) = s_m \exp(im\varphi) = s_m R^{im\mu} \exp(im\theta)$, $m \geq 0$. Then we show in the Appendix that

$$P(\varphi) = G s_m Y_m(\beta') e^{im\varphi}, \quad -\frac{1}{2}m < \beta < \frac{1}{2}(1+m). \quad (17)$$

where

$$\beta' \equiv \beta - \frac{1}{2}im\mu, \quad (18)$$

and (Kalnajs 1971)

$$Y_m(\beta') = \pi \frac{\Gamma\left(\frac{m}{2} - \beta' + \frac{1}{2}\right) \Gamma\left(\frac{m}{2} + \beta'\right)}{\Gamma\left(\frac{m}{2} - \beta' + 1\right) \Gamma\left(\frac{m}{2} + \beta' + \frac{1}{2}\right)}. \quad (19)$$

To determine the allowed range of β we first consider $m \neq 0$. For $m = 1$ the allowed range of β is $(-\frac{1}{2}, 1)$ (outside this range the force from material at $r \rightarrow \infty$ or $r \rightarrow 0$ diverges); for higher m the allowed range is broader.

The case $m = 0$ is special. The potential diverges and equation (19) does not apply unless $\beta \in (0, \frac{1}{2})$. However, it is easy to show that the total force arising from the surface density s_0 is finite throughout the larger range $\beta \in (-\frac{1}{2}, \frac{1}{2})$ and is given by

$$\mathbf{F} = -\nabla\Phi = -2\beta' R^{-2\beta'} G s_0 Y_0(\beta') \hat{\mathbf{e}}_R, \quad (20)$$

the same as predicted by equation (17). In other words the range of validity of equation (17) can be extended to $\beta \in (-\frac{1}{2}, \frac{1}{2})$ for $m = 0$ if it is only used to compute forces,

as in equations (15) and (16).

An additional constraint for warm discs ($k > 0$) is $\beta > -\frac{1}{4}$ so that pressure increases with density (equations 2 and 11), which ensures that sound waves are stable.

Henceforth we shall assume that β is restricted within the limits $(-\frac{1}{2}, \frac{1}{2})$ for cold discs and $(-\frac{1}{4}, \frac{1}{2})$ for warm discs.

3 LINEAR THEORY

We first examine the behaviour of scale-free discs that are slightly perturbed from axisymmetry.

3.1 Axisymmetric state

In an axisymmetric disc the variables are independent of the angle φ :

$$P(\varphi) = \frac{1}{2\beta}, \quad \bar{P} = \frac{f}{2\beta}, \quad Q(\varphi) = \frac{g}{2\beta}, \quad (21)$$

$$a(\varphi) = 0, \quad b(\varphi) = b_0, \quad S(\varphi) = c.$$

The notation is chosen so that the radial force from the axisymmetric disc is -1 at $R = 1$; the parameter $f \geq 0$ is the ratio of the force from the background potential to the force from the self-gravity of the disc. The surface density c is given by Poisson's equation (17):

$$2\beta G c Y_0(\beta) = 1. \quad (22)$$

The rotation speed b_0 is determined by equation (15):

$$b_0^2 = 1 + f - g. \quad (23)$$

The enthalpy is related to the surface density by the equation of state (12):

$$g = (1+4\beta)k c^{2\beta/(2\beta+1)}. \quad (24)$$

We parametrise the temperature of the disc by the inverse square of the Mach number (cf. equation 9),

$$w \equiv \frac{v_s^2}{b_0^2 R^{-2\beta}} = \frac{k}{b_0^2} \frac{1+4\beta}{1+2\beta} c^{2\beta/(2\beta+1)} = \frac{g}{b_0^2(1+2\beta)}. \quad (25)$$

We shall characterise axisymmetric discs with a given rotation parameter β by the parameter pair (w, f) , i.e. a measure of the temperature and a measure of the importance of the background potential. In terms of these parameters the rotation speed and enthalpy are given by

$$b_0^2 = \frac{1+f}{1+(1+2\beta)w}, \quad g = \frac{(1+2\beta)(1+f)w}{1+(1+2\beta)w} \quad (26)$$

where b_0^2 is given in terms of f and w by equation (26).

3.2 Response to potential perturbation

We impose a potential that is slightly perturbed from axisymmetry:

$$P_i(\varphi) = \frac{1}{2\beta} + p e^{im\varphi}, \quad (27)$$

with $p \ll 1$, and $m > 0$ an integer. We write the enthalpy as

$$Q(\varphi) = \frac{g}{2\beta} + q e^{im\varphi}, \quad (28)$$

and the velocity as

$$a(\varphi) = a_1 e^{im\varphi}, \quad b(\varphi) = b_0 + b_1 e^{im\varphi}, \quad (29)$$

from which equations (15) and (16) yield to first order

$$\begin{aligned} 2\beta'(p - q) - 2b_0 b_1 + im b_0 a_1 &= 0, \\ im(p - q) + b_0[(\beta - 1)a_1 - im b_1] &= 0, \end{aligned} \quad (30)$$

where β' is defined in equation (18). Equations (30) can be solved to find a_1 and b_1 in terms of p and q :

$$\begin{aligned} a_1 &= \frac{2im(p - q)(\beta' - 1)}{b_0[m^2 + 2(\beta - 1)]}, \\ b_1 &= \frac{(p - q)[m^2 + 2\beta'(\beta - 1)]}{b_0[m^2 + 2(\beta - 1)]}. \end{aligned} \quad (31)$$

The perturbed surface density may be written

$$S = c(1 + \sigma e^{im\varphi}) \quad (32)$$

and to first order equation (14) yields

$$(2\beta' + \beta)a_1 - im(b_1 + b_0\sigma) = 0. \quad (33)$$

From the equation of state (12) the perturbed enthalpy and surface density are related by

$$q = \frac{1 + 4\beta}{1 + 2\beta} k c^{2\beta/(2\beta+1)} \sigma; \quad (34)$$

using equations (24) and (26) we find the simpler form

$$q = b_0^2 w \sigma. \quad (35)$$

For a given unperturbed disc, specified by β , w , and f , and a given azimuthal wavenumber m , equations (31), (33) and (35) determine the surface density and velocity perturbations induced by the imposed potential p .

We now find the potential response to the perturbation, by applying equations (17) and (19) to equation (32):

$$P_r = Gc [Y_0(\beta) + Y_m(\beta') \sigma e^{im\varphi}]; \quad (36)$$

P_r is the response potential to the imposed potential perturbation P_i . Using equation (22) we may write equation (36) as

$$P_r = \frac{1}{2\beta} + A p e^{im\varphi}, \quad (37)$$

where we evaluate the Love number A using equations (22), (31), (33) and (35):

$$\frac{Y_m(\beta')}{2\beta Y_0(\beta)} = A b_0^2 \left[w - \frac{m^2 + 2(\beta - 1)}{m^2 + 2\beta + 2\beta' - 4\beta'^2} \right]. \quad (38)$$

If A is positive then the response potential supports the perturbing potential; if A is negative then the response potential is anti-aligned with the perturbing potential, and cannot support it. The special case $\beta = 0$ can be handled by taking the limit $\beta \rightarrow 0$ in equation (38).

3.3 Self-consistency

If the perturbation supports the potential, then it may be possible to construct a self-consistent disc, in which $P_r = P_i$. To do so we set $A = 1$, which requires

$$\frac{Y_m(\beta')}{2\beta Y_0(\beta)} = b_0^2 \left[w - \frac{m^2 + 2(\beta - 1)}{m^2 + 2\beta + 2\beta' - 4\beta'^2} \right]. \quad (39)$$

To analyse the solutions of (39) we write the equation as

$$B = b_0^2(w - C), \quad (40)$$

where b_0^2 is real but B and C may be complex. Thus we have

$$\Re(B) = b_0^2[w - \Re(C)], \quad \Im(B) = -b_0^2\Im(C). \quad (41)$$

The quantity $\Im(C)$ vanishes only if $\mu = 0$, or $\beta = \frac{1}{4}$ [or if $m^2 = 2(1 - \beta)$, but this cannot occur for $\beta \in (-\frac{1}{2}, \frac{1}{2})$]. Thus we have three families of solutions: (1) $\Im(C) = 0$, $\mu = 0$; (2) $\Im(C) \neq 0$; (3) $\Im(C) = 0$, $\beta = \frac{1}{4}$. We examine each family in turn.

3.3.1 Aligned discs ($\mu = 0$).

In this family the isodensity contours are aligned. The condition for self-consistency is derived by setting $\beta = \beta'$ in (39):

$$\frac{Y_m(\beta)}{2\beta Y_0(\beta)} = b_0^2 \left[w - \frac{m^2 + 2(\beta - 1)}{m^2 - 4\beta(\beta - 1)} \right]. \quad (42)$$

For a given rotation parameter β and azimuthal wavenumber m , equation (42) provides a unique relation between the Mach number (parametrised by w) and the background potential (parametrised by f) that support a non-axisymmetric stationary state; in other words the non-axisymmetric aligned discs are located on a curve in the (w, f) plane. Figures 1 and 2 plot solutions of equation (39) for various values of β and m .

The qualitative characteristics of these solutions are illuminated by examining special cases:

(i) Cold discs ($w = 0$). The left side of (42) is positive for all β , so self-consistency requires

$$\frac{m^2 + 2(\beta - 1)}{m^2 - 4\beta(\beta - 1)} < 0, \quad (43)$$

which is satisfied for $m > 0$ and $\beta \in (-\frac{1}{2}, \frac{1}{2})$ if and only if $m = 1$ and $\beta > -\frac{1}{2}(2^{1/2} - 1) = -0.2071$. A more stringent condition is that $f \geq 0$ since a repulsive background is unphysical; for $m = 1$ and $w = 0$, equation (42) yields $f \geq 0$ only when $\beta \geq 0$. Thus cold, non-axisymmetric stationary states can only exist if $m = 1$ and $\beta \geq 0$.

(ii) Low-mass discs ($f \rightarrow \infty$). In this case the quantity in square brackets in equation (42) must be zero, which requires

$$w = \frac{m^2 + 2(\beta - 1)}{m^2 - 4\beta(\beta - 1)}; \quad (44)$$

since $w \geq 0$, stationary non-axisymmetric discs with negligible mass exist if and only if the inequality (43) is *not* satisfied; in other words if and only if $m \geq 2$ or $\beta < -\frac{1}{2}(2^{1/2} - 1) = -0.2071$. A corollary is that for $m = 1$ and $\beta > -0.2071$, f is always finite; i.e. the disc always has significant self-gravity.

(iii) Non-rotating discs ($w \rightarrow \infty$). In this case

$$f = \frac{(1 + 2\beta)Y_m(\beta)}{2\beta Y_0(\beta)} - 1. \quad (45)$$

For $m = 1$ the condition $f \geq 0$ requires $\beta \leq 0$. For $m \geq 2$ equation (45) yields unphysical solutions ($f < 0$) for all β .

(iv) Flat rotation curve ($\beta = 0$). We may evaluate (42) using the relation $\Gamma(x) \sim x^{-1}$ as $x \rightarrow 0$; in particular for $m = 1$ we find the simple result that

$$f = 0 \quad \text{for } \beta = 0, \quad \text{and all } w; \quad (46)$$

in other words isolated discs with a flat rotation curve support a neutral $m = 1$ mode for any Mach number.

Comparison of (iii) with (i) shows that the $m = 1$ solution curve in the (w, f) plane must cross $f = 0$ for all rotation parameters β ; the location of this crossing point (i.e. the value of w that supports isolated non-axisymmetric discs) is shown in Figure 2.

3.3.2 Spiral discs ($\mu > 0$)

These are discs with self-similar spiral patterns. In equation (41), $\Im(C) \neq 0$. Equation (39) has real and imaginary parts. Thus, once β and m are specified, there are two equations for three unknowns (w, f, μ) . Therefore the spiral discs are located on a curve in the (w, f) plane parametrised by the value of μ . The aligned and the spiral sequences are plotted in Figure 1.

The spiral sequence bifurcates from the sequence of aligned discs at the point where $\mu \rightarrow 0$. The location of the bifurcation point can be determined analytically. For small μ we can replace $\Im(B)$ by $-\frac{1}{2}im\mu(\partial B/\partial\beta')$ where the derivative is evaluated at $\mu = 0$, with a similar expression for $\Im(C)$. Thus at the bifurcation point, the equilibrium equations (41) simplify to

$$B = b_0^2(w - C), \quad \frac{\partial B}{\partial\beta'} = -b_0^2 \frac{\partial C}{\partial\beta'}, \quad (47)$$

where all quantities are evaluated at $\mu = 0$ ($\beta = \beta'$). Eliminating b_0 , we find

$$\frac{\partial \log B}{\partial\beta'} = \frac{\partial \log(w - C)}{\partial\beta'}; \quad (48)$$

the derivatives are taken with β , f and w fixed. Evaluating this expression yields

$$w = \frac{2(1 - 4\beta)[m^2 + 2(\beta - 1)]}{[m^2 + 4\beta(1 - \beta)]^2 \Psi_m(\beta)} + \frac{m^2 + 2(\beta - 1)}{m^2 + 4\beta(1 - \beta)}, \quad (49)$$

where

$$\Psi_m(z) \equiv \psi\left(\frac{1}{2}m + z\right) + \psi\left(\frac{1}{2}m - z + 1\right) - \psi\left(\frac{1}{2}m + z + \frac{1}{2}\right) - \psi\left(\frac{1}{2}m - z + \frac{1}{2}\right) \quad (50)$$

and $\psi(z)$ is the digamma function. This expression defines w at the bifurcation point; the other coordinate f then follows from (42). The expression (49) is singular for $m = 1$ at $\beta = -\frac{1}{2}(2^{1/2} - 1) = -0.2071$, $f = 0.4381$.

The location of the bifurcation point is plotted in Figure 3 for $m = 1$. For $m \geq 2$ the bifurcation point is unphysical ($f < 0$) for all β .

The equation governing self-similar spiral patterns simplifies in the WKB limit ($\mu \gg 1$). Using the asymptotic properties of the Gamma function we may show that in this limit

$$Y_m(\beta') = Y_m\left(\beta + \frac{1}{2}m\mu\right) = \frac{2\pi}{m\mu} \left(1 + \frac{2\beta - \frac{1}{2}}{im\mu}\right) + O(\mu^{-3}); \quad (51)$$

thus the dominant real and imaginary parts of equation (39) become respectively

$$\frac{\pi}{\beta Y_0(\beta)} = m\mu b_0^2 \left[w - \frac{m^2 + 2(\beta - 1)}{m^2 \mu^2} \right], \quad (52)$$

$$\frac{\pi}{\beta Y_0(\beta)} = -\frac{2b_0^2}{m\mu} [m^2 + 2(\beta - 1)].$$

Taking the ratio of these two equations yields

$$w \rightarrow \frac{2(1 - \beta) - m^2}{m^2 \mu^2} \quad \text{as } \mu \rightarrow \infty. \quad (53)$$

Similarly,

$$f \rightarrow \frac{\pi}{2\beta Y_0(\beta)} \left[\frac{m\mu}{2(1 - \beta) - m^2} \right] \quad \text{as } \mu \rightarrow \infty. \quad (54)$$

Thus $w \rightarrow 0$ and $f \rightarrow \infty$ as $\mu \rightarrow \infty$; in other words the WKB limit applies only if discs are cold and the background dominates the unperturbed potential. Moreover the WKB solution is unphysical for $m \geq 2$ since these equations imply that w and f are negative. Equations (53) and (54) can also be combined to eliminate μ :

$$wf^2 = \left[\frac{\pi}{2\beta Y_0(\beta)} \right]^2 \frac{1}{2(1 - \beta) - m^2}, \quad w \ll 1, \quad f \gg 1. \quad (55)$$

It is informative to relate the properties of these discs to the usual WKB spiral density waves in a fluid disc (e.g. Goldreich & Tremaine 1979). The dispersion relation for these waves has two branches (“long” and “short” waves) so a typical disc can support zero, one, or two wavetrains at any point. Why then do self-similar spiral patterns only exist in discs satisfying the constraint (55)? Consider a self-similar disc with unperturbed surface density $\propto R^{-2\beta-1}$. In this disc, linear WKB density waves with zero pattern speed are also self-similar, but the surface density perturbation associated with the waves is generally $\propto R^{-3/2}$, a result which follows from conservation of angular momentum flux (e.g. Goldreich & Tremaine 1979). Thus the fractional density perturbation is $\propto R^{-2\beta+1/2}$, which is not independent of radius, so the combination of axisymmetric disc and density wave is not self-similar. The only exceptions are (i) $\beta = \frac{1}{4}$, a case which we examine below; (ii) waves with zero angular momentum flux, the condition for the existence of which can be shown to be the same as (55).

We have seen that both the start of the spiral sequence ($\mu = 0^+$) and the asymptotic limit of the sequence ($\mu \rightarrow \infty$) lie in unphysical regions of the (w, f) plane ($w < 0$ or $f < 0$) when $m \geq 2$. These results suggest that the entire spiral sequence is unphysical when $m \geq 2$. We have not been able to prove this conjecture, but a numerical search has not revealed any counter-examples.

3.3.3 $\beta = \frac{1}{4}$ discs

The condition for self-consistency can be written

$$\left| \frac{\Gamma\left(\frac{1}{2}m + \frac{1}{4} + \frac{1}{2}im\mu\right)\Gamma\left(\frac{3}{4}\right)}{\Gamma\left(\frac{1}{2}m + \frac{3}{4} + \frac{1}{2}im\mu\right)\Gamma\left(\frac{1}{4}\right)} \right|^2 = \frac{1+f}{2+3w} \left[w + \frac{\frac{3}{2} - m^2}{m^2 + \frac{3}{4} + m^2 \mu^2} \right]. \quad (56)$$

For this particular value of β , equation (39) is real for all μ . Once m is specified, there is one equation for three unknowns

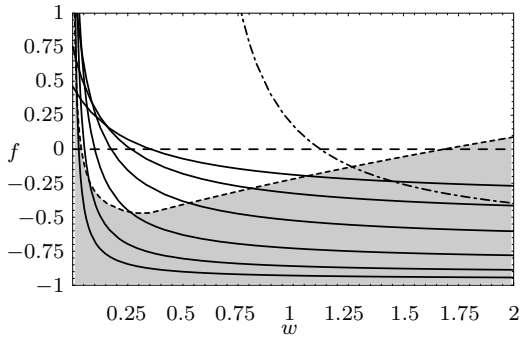


Figure 4. As in Figure 1, for a disc with $\beta = \frac{1}{4}$. The solid curves show the loci of solutions with $m = 1$; from top to bottom at large w : $\mu = 0, 1, 2, 4, 8, 16$. The dot-dashed curve shows $m = 2$ and $\mu = 0$. For $m = 2$ and $\mu > 0$ spiral solutions are unphysical because $w < 0$; the region below the dashed line at $f = 0$ is also unphysical. In the shaded region the axisymmetric disc is subject to an $m = 0$ instability.

(w, f, μ) . Thus the spiral discs are located on a set of curves in the (w, f) plane labelled by the value of μ . Self-similar spiral discs with $m = 1$ are not restricted to a single curve in the (w, f) plane: instead they occupy a two-dimensional area, as shown in Figure 4.

3.4 Stability

The linear stability of axisymmetric scale-free discs to axisymmetric disturbances has been investigated by Lemos *et al.* (1991). Their analysis is based on the observation that the squared eigenfrequency of axisymmetric modes is real, so that neutral modes mark the boundary between stable and unstable modes (Lynden-Bell & Ostriker 1967). Thus their calculations are quite similar to ours, except that they focus on the azimuthal wavenumber $m = 0$, whereas our analysis beyond equation (36) is only valid for $m > 0$. We may extend our analysis to the axisymmetric case by replacing $\exp(im\varphi)$ in equations (27), (28), (29), (32) and (36) by $\exp(i\nu \log R)$ and carrying out a slightly more careful derivation using Lagrangian perturbations. In our notation, the condition for a neutral, self-similar, axisymmetric disturbance is (cf. equation 39)

$$\frac{Y_0(\beta')}{2\beta Y_0(\beta)} = b_0^2 \left[w - \frac{\beta - 1}{\beta' - 2\beta'^2} \right]; \quad (57)$$

where $\beta' = \beta - \frac{1}{2}i\nu$. Since we are only investigating stability rather than constructing a self-similar non-axisymmetric disk, the fractional amplitude of the perturbation need not be independent of radius; thus β' can be an arbitrary complex number with $0 < \Re(\beta') < \frac{1}{2}$ (equation 17). Following Lemos *et al.* (1991), we focus on $\Re(\beta') = \frac{1}{4}$, for which both sides of equation (57) are real, although roots with other values of $\Re(\beta')$ may exist.

The location of the stability boundaries in the (w, f) plane can be determined by the following argument. Let $\beta' = \frac{1}{4} - \frac{1}{2}i\alpha$, where α is real, and rewrite (57) in the form

$$F(\alpha) \equiv B(\alpha) - b_0^2[w - C(\alpha)] = 0 \quad (58)$$

where

$$B(\alpha) \equiv \frac{\pi |\Gamma(\frac{1}{4} - \frac{1}{2}i\alpha)|^2}{2\beta Y_0(\beta) |\Gamma(\frac{3}{4} + \frac{1}{2}i\alpha)|^2}, \quad (59)$$

and

$$C(\alpha) \equiv \frac{2(\beta - 1)}{\frac{1}{4} + \alpha^2}. \quad (60)$$

Since $F(\alpha)$ is even, it must have an even number of roots. The stability boundary is marked by the transition from zero roots to two roots, which occurs when

$$F(\alpha) = B(\alpha) - b_0^2[w - C(\alpha)] = 0, \quad (61)$$

$$F'(\alpha) = B'(\alpha) + b_0^2 C'(\alpha) = 0$$

simultaneously for some α . Eliminating b_0 , we have

$$\frac{d \log B(\alpha)}{d\alpha} = \frac{d \log [w - C(\alpha)]}{d\alpha}, \quad (62)$$

which yields

$$i\Psi_0(\frac{1}{4} - \frac{1}{2}i\alpha) = \frac{8(1 - \beta)\alpha}{(\frac{1}{4} + \alpha^2)[(\frac{1}{4} + \alpha^2)w + 2(1 - \beta)]}, \quad (63)$$

where $\Psi_m(z)$ is defined in equation (50) and both sides are real. To locate the stability boundaries we distinguish two cases: (i) if $\alpha = 0$ equation (63) is satisfied, and the corresponding stability boundary on the (w, f) plane is found by solving $F(0) = 0$ for f as a function of w ; (ii) if $\alpha \neq 0$ we can easily manipulate (63) to solve for $w(\alpha)$ and then use $F(\alpha) = 0$ to find f as a function of α and $w(\alpha)$. Figures 1, 2, and 4 show the regions where $m = 0$ instabilities are present in the (w, f) plane.

The close relation between neutral modes and the onset of axisymmetric instability does not extend to non-axisymmetric disturbances (e.g. Lynden-Bell & Ostriker 1967). However, non-axisymmetric neutral modes would mark the stability boundary for systems composed of two equal, counter-rotating discs (we imagine that the discs interact only through their mutual gravity), since in this case the equilibrium is time-reversal invariant. Thus analyses similar to that of Lemos *et al.* could illuminate non-axisymmetric two-stream instabilities in scale-free counter-rotating discs (Araki 1987, Sellwood & Merritt 1994).

4 NONLINEAR THEORY

We may extend our analysis to nonlinear departures from axisymmetry by expanding all the disc properties in a Fourier series, truncating the series, and solving the resulting nonlinear equations for the Fourier coefficients by Newton's method. For a given rotation parameter β and background potential f , we expect to have a sequence of solutions with m -fold symmetry in which the Mach number parameter w is a function of the amplitude

$$Z \equiv S(\pi)/S(0) - 1, \quad (64)$$

where zero azimuth is chosen so that $Z > 0$. In the limit $Z \rightarrow 0$, w is determined by the linear theory of Section 3.

We have restricted our numerical calculations to aligned discs. Thus we set

$$S(\theta) = c \left[1 + \sum_{k=1}^n s_k \cos(km\theta) \right] \quad (65)$$

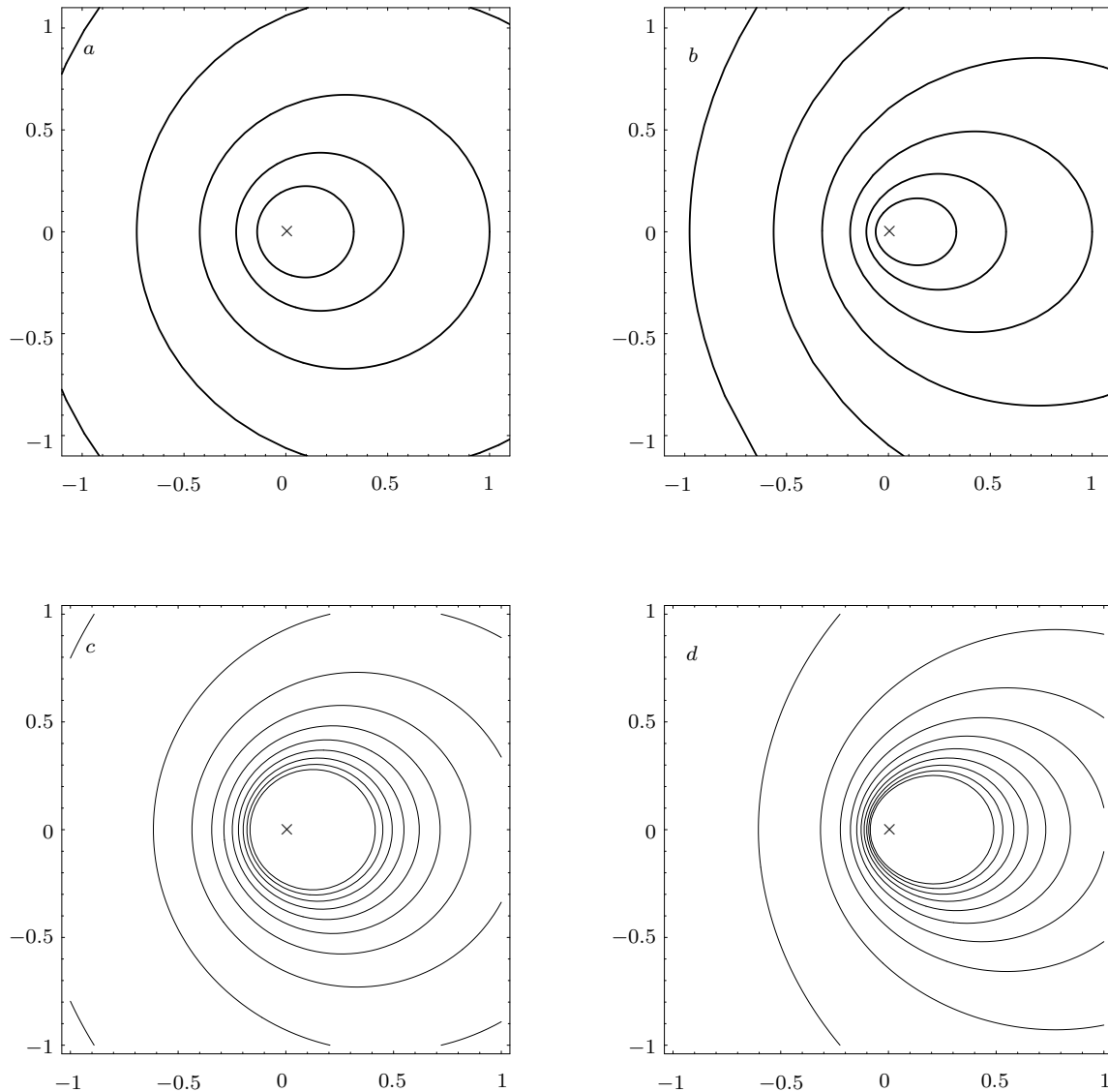


Figure 5. Cold non-axisymmetric discs with $\beta = 0.33$. a) and b) show streamlines for density contrast $Z = 2.333$ and $Z = 9$ respectively. (c) and (d) show density contours for those discs.

$$a(\theta) = \sum_{k=1}^n a_k \sin(km\theta), \quad b(\theta) = b_0 + \sum_{k=1}^n b_k \cos(km\theta) \quad (66)$$

and truncate all the series at order n . The potential of the disc is given by

$$P(\theta) = Gc \left[Y_0(\beta) + \sum_{k=1}^n Y_{km}(\beta) s_k \cos(km\theta) \right], \quad (67)$$

and the enthalpy is

$$Q(\theta) = \frac{g}{2\beta} + \sum_{k=1}^n q_k \cos(km\theta). \quad (68)$$

For computational convenience we work with warm discs whose rotation parameters have the form $\beta = \frac{1}{2}(\ell - 1)^{-1}$, where ℓ is an integer (e.g. $\beta = \frac{1}{4}, \frac{1}{6}, \frac{1}{8}, \dots$) since (12) then implies that $S \propto Q^\ell$, which is easier to evaluate if ℓ is an integer. The solutions are parametrised by the value of Z .

Figure 5 shows streamlines and density contours for two cold discs with $\beta = 0.33$, using $m = 1$, $n = 5$. The first has $Z = 2.333$ and $f = 0.658$. The second has $Z = 9$ and $f = 0.816$. For comparison, linear theory predicts $f = 0.604$.

Figure 6 shows streamlines and density contours for two isolated ($f = 0$) warm discs with $\beta = \frac{1}{4}$, using $m = 1$ and $n = 10$. The first has $Z = 2.333$ and $w = 0.355$. The second has $Z = 9$ and $w = 0.349$ (linear theory predicts $w = 0.353$).

Figure 7 shows streamlines and density contours for two isolated ($f = 0$) cold discs with $\beta = 0$, using $m = 1$ and $n = 10$. The first has $Z = 1$; the second has $Z = 2.333$.

5 DISCUSSION

We have sought non-axisymmetric equilibrium states of scale-free razor-thin discs of a two-dimensional barotropic fluid embedded in an axisymmetric background potential. The rotation curves of the discs have the form $v \propto R^{-\beta}$, $\beta \in (-\frac{1}{2}, \frac{1}{2})$ for cold discs and $\beta \in (-\frac{1}{4}, \frac{1}{2})$ for warm

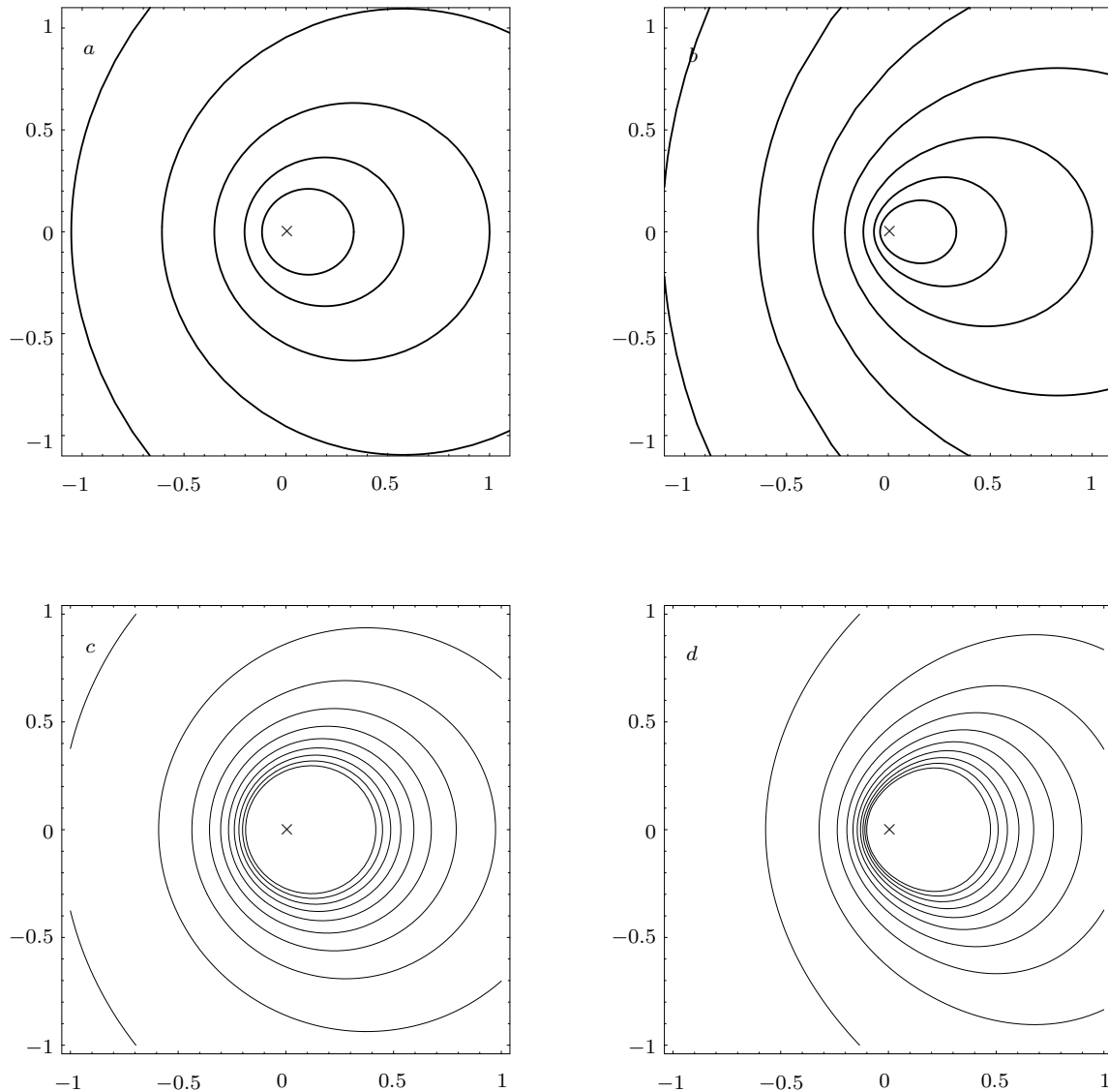


Figure 6. Warm isolated discs ($f = 0$) with $\beta = \frac{1}{4}$. (a) and (b) show streamlines for $Z = 2.333$ and $Z = 9$ respectively. (c) and (d) show density contours for those discs.

barotropic discs. The discs are specified by the rotation parameter β , the inverse-square Mach number $w > 0$, and the ratio of the force from the background to the force from the unperturbed disc, $f > 0$. For small departures from axisymmetry, we have found that:

- (i) In cold or cool discs ($w \ll 1$), stationary equilibrium states exist only for lopsided modes ($m = 1$) and for rotation parameters $\beta \geq -\frac{1}{2}(2^{1/2} - 1) = -0.2071$.
- (ii) For most values of β , stationary equilibrium states exist only along two sequences in the (w, f) plane: the aligned discs and the spiral discs. The spiral-disc sequence bifurcates from the aligned-disc sequence. We have argued that the spiral-disc sequence is only physical if $m = 1$.
- (iii) Isolated ($f = 0$) discs with flat rotation curves ($\beta = 0$) support non-axisymmetric equilibrium states for all values of the Mach number.
- (iv) Discs with $\beta = \frac{1}{4}$ support $m = 1$ spiral equilibrium states not just along a single sequence but over a large

part of the (w, f) plane.

We have also constructed equilibria with large departures from axisymmetry (range of surface density at a given radius of a factor ten).

The rotation curves of our models have the characteristic feature that they are asymmetric along the long axis. The rotation velocity is high where the surface density is low. Similar features are seen in the rotation curves of Magellanic irregulars (de Vaucouleurs & Freeman 1972). Other lopsided galaxies, such as NGC 891, where the gas distribution extends much further on one side than the other, have symmetric rotation curves (Sancisi & Allen, 1979). In NGC 891 the stellar distribution is also very symmetric. Our models do not reproduce this behaviour.

It would be interesting to construct stellar dynamic equivalents of our fluid models. There is no general argument which guarantees that such models exist. However, the cold fluid discs we have constructed are also valid models for cold stellar discs; also, the case $\beta = 0$, $m = 2$ has been

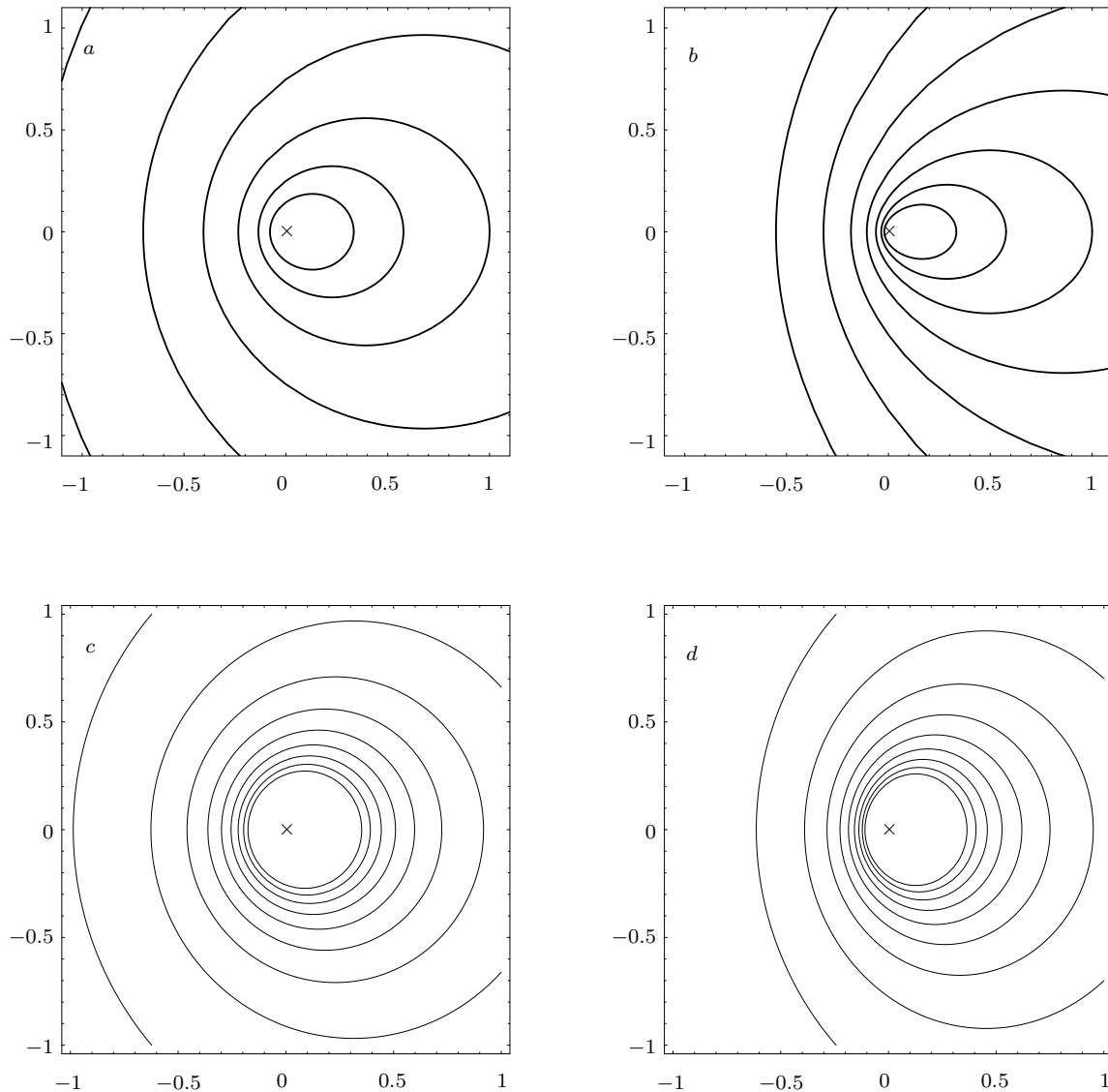


Figure 7. Cold isolated discs with $\beta = 0$. a) and b) show streamlines for $Z = 1$ and $Z = 2.333$ respectively. (c) and (d) show density contours for those discs.

studied by Kuijken (1993), and a number of hot models were constructed.

This research was supported by NSERC and PPARC.

REFERENCES

- Araki, S. 1987, *AJ*, 94, 99
 Baldwin, J., Lynden-Bell, D., & Sancisi, R. 1980, *MNRAS*, 193, 313
 de Vaucouleurs, G., and Freeman, K.C. 1972, *Vistas in Astronomy*, 16, 163
 Goldreich, P., & Tremaine, S. 1979, *ApJ*, 233, 857
 Richter, O.-G., & Sancisi, R. 1994, *AA*, 290, L9
 Kalnajs, A. J. 1971, *ApJ*, 166, 275
 Kuijken, K. 1993, *ApJ*, 409, 68
 Lemos, J.P.S., Kalnajs, A. J., & Lynden-Bell, D. 1991, *ApJ*, 375, 484
 Lynden-Bell, D., & Ostriker, J. P. 1967, *MNRAS*, 136, 293
 Qian, E. 1992, *MNRAS*, 257, 581

- Rix, H-W., & Zaritsky, D. 1995, *ApJ*, 447, 82
 Sellwood, J. A., & Merritt, D. 1994, *ApJ*, 425, 530
 Sancisi, R., & Allen, R. J. 1979, *AA*, 74, 73
 Weinberg, M. D. 1983, *ApJ*, 271, 595
 Weinberg, M. D. & Tremaine, S. 1983, *ApJ*, 271, 586

APPENDIX

We wish to derive the potential arising from a surface density of the form

$$\Sigma(R, \theta) = R^\alpha e^{im\theta}. \quad (69)$$

We begin with the potential-density pair (Qian 1992)

$$\Sigma_b(R, \theta) = \frac{(m + \frac{1}{2})}{\pi b^2} \left(\frac{R}{b}\right)^m \frac{e^{im\theta}}{(1 + R^2/b^2)^{m+3/2}}, \quad (70)$$

$$\Phi_b(R, \theta) = -\frac{G}{b} \left(\frac{R}{b}\right)^m \frac{e^{im\theta}}{(1 + R^2/b^2)^{m+1/2}}.$$

We now form the scale-free density-potential pair

$$\int_0^\infty b^{\alpha+1} \Sigma_b(R, \theta) db; \quad \int_0^\infty b^{\alpha+1} \Phi_b(R, \theta) db; \quad (71)$$

both integrals converge so long as $-m - 2 < \Re(\alpha) < m - 1$, and yield

$$\begin{aligned} & \frac{1}{2\pi} R^\alpha e^{im\theta} \frac{\Gamma(\frac{1}{2}m + \frac{1}{2}\alpha + \frac{3}{2})\Gamma(\frac{1}{2}m - \frac{1}{2}\alpha)}{\Gamma(m + \frac{1}{2})}; \\ & - \frac{G}{2} R^{\alpha+1} e^{im\theta} \frac{\Gamma(\frac{1}{2}m + \frac{1}{2}\alpha + 1)\Gamma(\frac{1}{2}m - \frac{1}{2}\alpha - \frac{1}{2})}{\Gamma(m + \frac{1}{2})}. \end{aligned} \quad (72)$$

Thus the potential corresponding to the surface density (69) is (Kalnajs 1971)

$$\begin{aligned} \Phi(R, \theta) = & -\pi G R^{\alpha+1} e^{im\theta} \\ & \times \frac{\Gamma(\frac{1}{2}m + \frac{1}{2}\alpha + 1)\Gamma(\frac{1}{2}m - \frac{1}{2}\alpha - \frac{1}{2})}{\Gamma(\frac{1}{2}m + \frac{1}{2}\alpha + \frac{3}{2})\Gamma(\frac{1}{2}m - \frac{1}{2}\alpha)}, \end{aligned} \quad (73)$$

where $-m - 2 < \Re(\alpha) < m - 1$.

This paper has been produced using the Blackwell Scientific Publications \TeX macros.